Reactivity of Tetracyclic Iminium Salts of the Benzo[*f*]pyrido[2,1-*a*]-isoindole and Azepino[2,1-*a*]benzo[*f*]isoindole Type, with a Preliminary Analysis of their Interactions with Nucleic Acids*

Gerhard Maas[a], Hans-Georg Herz[a], Elke Scheppach[a], Barbara Susanne Palm[b], and Hans-Jörg Schneider[b]

[a] Abteilung Organische Chemie I, Universität Ulm, Albert-Einstein-Allee 11, D-89081 Ulm, Germany
[b] FR Organische Chemie, Universität des Saarlandes, D-66041 Saarbrücken, Germany

Reprint requests to Prof. Dr. G. Maas. Fax: +49(731)5022803.
E-mail: gerhard.maas@chemie.uni-ulm.de

Z. Naturforsch. **59b,** 486 – 497 (2004); received February 10, 2004

Hydride reduction of the tetracyclic isoindolium salt derivatives **2a – c** yields the neutral isoindole derivatives 9-chloro-1,2,3,4,6,6a,7,12b-octahydrobenzo[*f*]pyrido[2,1-*a*]isoindole (**3a**), 4,4a,5,7,8,9,10,10a-octahydropyrido[2,1-a]thieno[3,2-f]isoindole (**3b**), and 10-chloro-2,3,4,5,7,7a,8,13b-octahydro-1*H*-azepino[*f*]pyrido[2,1-*a*]isoindole (**3c**). Oxidation of **3a** with selenium dioxide is accompanied by a ring transformation and yields 8-chloro-5,5a,6,12-tetrahydrobenzo[*g*]pyrrolo[1,2-*b*]isoquinolin-12-one (**4**). Deprotonation of isoindolium salt derivatives **2a**,**c**,**d** yields cyclic enamines which undergo ring expansion with dimethyl acetylenedicarboxylate resulting in compounds with the 4,5,6,8,8a,9-hexahydroazocino[2,1-*a*]benzo[*f*]isoindole (**6a**), 4,6,7,9,9a,10-hexahydro-5*H*-azonino[2,1-*a*]benzo[*f*]isoindole (**6c**) and 4a,5,7,8,9,10-hexahydro-4*H*-azonino[2,1-*a*]thieno[3,2-*f*]isoindole (**6d**) skeleton. Interactions of **2** with double-stranded nucleic acids are characterized by relatively large NMR upfield shifts (0.25 ppm) and signal broadening (by about 45 Hz) of aromatic ligand signals, indicating at least partial stacking with nucleobases. Rather small effects are observed, however, in melting point and viscosity increase with double strands; this is tentatively ascribed to competitive interactions with unfolded polymer parts.

Key words: Azaheterocycles, Iminium Salts, Enamines, Isoindole Derivatives, DNA Binding

Introduction

We have reported recently that *N*-allyl-2-(het)arylethynyl-3,4,5,6-tetrahydropyridinium triflates (**1**, $n = 1$) and *N*-allyl-2-(het)arylethynyl-4,5,6,7-tetrahydro-3*H*-azepinium triflates (**1**, $n = 2$) undergo a thermally induced intramolecular [4+2] cycloaddition reaction which after a hydrogen shift provides the tetracyclic isoindolium derivatives **2** [1]. The presence of a reactive iminium function in these fused ring systems offers opportunities for further synthetic modifications leading in particular to neutral heterocyclic systems with a nitrogen atom at a ring fusion position. Structural moieties of this type are incorporated in a variety of biologically important alkaloids including

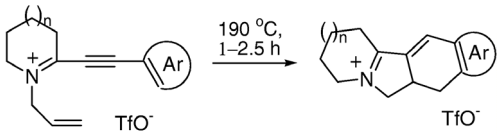

1 **2**

n = 1,2
Ar = 4-chlorophenyl, 2-thienyl

Scheme 1. Thermally induced intramolecular cycloisomerization of **1**.

those of the pyrrolizidine (5-5 fused ring systems) [2], indolizidine (6-5) [3] and quinolizidine (6-6) [4] classes.

In this paper, some transformations of the cationic isoindole derivatives **1** are reported that make use of two of the most important transformations of an iminium function, namely conversion into amines by hydride addition and into enamines by α-deprotona-

* Presented in part at the 6th Conference on Iminium Salts (ImSat-6), Stimpfach-Rechenberg (Germany), September 16 – 18, 2003.

tion. In addition, the ability of the rather flat tetracyclic iminium salts **2** to intercalate with DNA is briefly discussed.

Results and Discussion

*Hydride reduction of iminium salts **2a – c***

Salts **2a – c** were converted into the neutral tetracyclic isoindole derivatives **3a – c** by reduction with $LiAlH_4$ in 56 – 69% yield (Scheme 1). Distinctly lower yields were obtained with $NaBH_4$ and $NaBH_3CN$, respectively. The $LiAlH_4$ reduction of cyclic iminium salts has recently been used in a general method to prepare 1-azabicyclo[m.n.0]alkanes [5]. Hydride addition at the iminium carbon atom of **2a – c** generates a second stereogenic center. The NMR spectra of **3a** and **3b** indicate the presence of two stereoisomers, while in the case of azepino[2,1-*a*]isoindole derivative **3c**, one isomer was formed exclusively or nearly so (the ^1H and ^{13}C NMR spectra show trace amounts of a second compound which disappears on recrystallization).

Although the ^1H and ^{13}C NMR chemical shifts (Table 1 and Chart 1) could be readily assigned based mainly on H,H and C,H correlation spectra, extensive signal overlap in the aliphatic region and broadening of some signals did not allow to establish the relative stereochemistry of these compounds in a straightforward manner. It must be kept in mind that (partially) saturated fused heterocycles with a nitrogen atom at a ring fusion position in many cases are subject to conformational equilibria which are caused by ring inversion and/or nitrogen inversion [6, 7]. For example, nitrogen inversion transforms the trans-fused six-membered rings of the quinolizidine (1-azabicyclo[4.4.0]decane) system into a cis-fused arrangement; while the trans-bis-chair conformer is much more stable than the cis-bis-chair conformer in the case of the parent system [6, 7] and all monomethyl-quinolizidines exist predominantly in the trans-fused ring conformation [8], cis-fused conformations are well known for various other substituted quinolizidines [6, 8]. Conformational analysis has been carried out for a number of natural and synthetic alkaloids featuring a nitrogen atom at a ring fusion position. Recent examples include substituted quinolizidines (6-6 fused azabicyclic ring systems) [9], perhydropyrido[1,2-*c*]1,3-oxazepines (6-6 systems) [10], berbines (5,6,13,13a-tetrahydro-8*H*-dibenzo[*a*,*g*]quinolizines, 6-6 systems) [11], B- and C-homoberbines (hexahydroisoquinobenzazepines, 7-6 systems) [12], 3,4,10,10a-tetrahydro-1*H*-[1,4]oxazino[4,3-*a*]azepines (7-6 systems) [13] and octahydropyrido[1,2-*b*][2]benzazonines, (9-6 systems) [14].

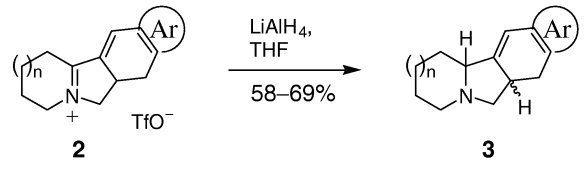

2 **3**

2,3	a	b	c
n	1	1	2
	Ar, Cl	S	Cl
d.r.	72:28	17:83	>95:5

Scheme 2. Hydride reduction of cyclic iminium salts **2**.

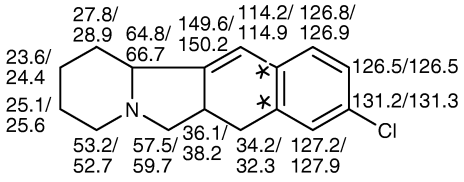

3a[a] ✳ 133.5/133.9 and 136.8/137.0

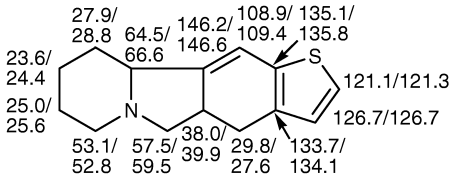

3b[b]

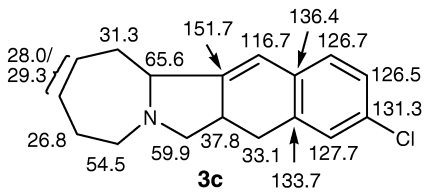

3c

[a] Two isomers; **A** (first value) / **B** = 72/28; [b] two isomers; **A** (first value) / **B** = 17/83.

Chart 1. ^{13}C chemical shifts ($CDCl_3$, 125.77 MHz, δ values (ppm)) of compounds **3a – c**.

The relative stereochemistry of compounds **3a** and **3c** could be established by crystal structure analysis. Suitable crystals of **3a** were obtained by fractionating crystallization from an acetonitrile-acetone mix-

Table 1. ^{1}H NMR data of compounds **3a – c** (500.13 MHz, $CDCl_3$, 306 K, δ (ppm), J (Hz))[a].

	3aA	**3aB**		**3bA**	**3bB**	**3c**		
							306 K	253 K
1-H	1.32 – 1.44 m 1.95 – 2.09 m	1.36 – 1.44 m 1.95 – 2.09 m	10-H	1.29 – 1.40 m 1.86 – 2.01 m	1.18 – 1.46 m 1.86 – 2.07 m	1-H	1.59 – 1.68 m 1.72 – 1.78 m	1.62 – 1.75 m
2-H	1.25 – 1.40 m 1.80 – 1.91 m	1.25 – 1.40 m 1.80 – 1.91 m	9-H	1.23 – 1.37 m 1.75 – 1.87 m	1.21 – 1.42 m 1.72 – 1.93 m	2-H	1.45 – 1.54 m 1.80 – 1.89 m	1.40 – 1.47 m 1.80 – 1.95 m[b]
3-H	1.57 – 1.72 m	1.57 – 1.72 m	8-H	1.50 – 1.64 m	1.49 – 1.69 m	3-H	1.45 – 1.54 m 1.80 – 1.89 m	1.40 – 1.47 m 1.80 – 1.95 m[b]
						4-H	1.55 – 1.62 m 1.80 – 1.88 m	1.58 – 1.70 m 1.82 – 1.92 m
4-H	2.14 – 2.26 m 3.02 – 3.11 dt (^2J = 10.5)	2.14 – 2.26 m 3.11 – 3.16 br d (^2J = 10.6)	7-H	2.02 – 2.28 m 3.04 dt (^2J = 10.3)	2.02 – 2.28 m 3.11 dt (^2J = 10.7)	5-H	2.75 ddd (J = 12.5, 8.3, 2.1) 2.94 – 3.00 m	2.61 dd[c] 3.18 dd[c]
6-H	2.59 t (J = 9.0) 2.92 dd (J = 9.4, 2.0)	2.02 – 2.08 m 3.27 – 3.33 pt	5-H	2.58 t (J = 8.3) 2.79 – 2.93	2.07 dd (J = 9.8, 8.2) 3.26 pt	7-H	2.61 t (J = 8.5) 3.10 t (J = 8.4)	2.46 t (J = 9.2) 3.24 dd[c]
6a-H	2.76 – 2.88 m	2.76 – 2.83 m	4a-H	2.83 – 3.04 m	2.83 – 3.04 m	7a-H	2.89 – 2.96 m	2.90 – 3.00 m
7-H	2.70 – 2.83 m	2.53 t (J = 16.8) 2.77 d (J = 16.8)	4-H	2.50 – 2.61 2.86 – 2.90	2.39 t 2.84 t	8-H	2.60 br t (J = 15.0) 2.82 dd (J = 15.0, 6.6)	2.57 t (J = 15.4) 2.89 dd (J = 15.0, 6.5)
8-H, 10-H	7.05 – 7.11	7.05 – 7.11	3-H 2-H	6.80 d (J = 5.0) 6.99 d (J = 5.0)	6.81 d (J = 5.0) + 7.01 d (J = 5.0)	9-H, 11-H	7.08 – 7.12	7.13 – 7.16 m
11-H	6.94 d	6.94 d				12-H	6.93 d (J = 7.9)	7.00 d (J = 8.0)
12-H	6.11 br s	6.15 br s	11-H	6.14 t (J = 2.5)	6.18 t (J = 2.7)	13-H	6.16 t (J = 2.5)	6.24 br s
12b-H	2.54 – 2.62	2.66 – 2.72 br d (J = 10.0)	10a-H	2.58 t	2.69 br d (J = 8.5)	13b-H	3.70 dd (J = 9.6, 1.8)	3.91 br d (J = 8.3)

[a] Due to signal overlap, multiplicities of some signals cannot be recognized; br = broadened, pt = pseudo-triplet; [b] marked assignments for protons 2-H and 3-H may be interchanged; [c] coupling constants could not be determined accurately due to line overlap or signal broadening.

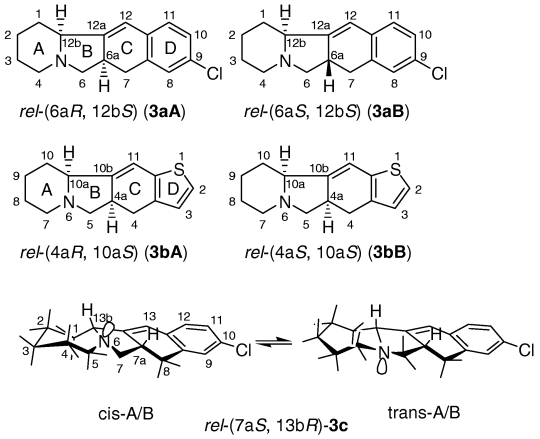

Scheme 3. Observed stereoisomers and numbering system of compounds **3a – c**.

ture. The ^{1}H NMR spectrum of the first-formed crystal batch indicated that the two isomers **A** and **B** were still present but that the composition had changed from 72:28 to 82:18; on extended standing, some more material crystallized which was enriched in isomer **B** (25:75 mixture). The structure determination was carried out on a crystal from the first batch, and the result is shown in Fig. 1. A partially disordered structure with unequal site occcupation factors was found, the values of the latter matching very closely the **A**:**B** ratio of the crystal batch as measured by ^{1}H NMR. This means that isomers **A** and **B** are incorporated in the same crystal lattice and that the major isomer (**A**) seen by ^{1}H NMR of the product mixture is also the major component in the crystal. The two components of the crystal structure are diastereomers: isomer **A** has the cis(6a-H, 12b-H) and **B** the trans(6a-H, 12b-H) configuration. In other words, major isomer **3aA** has the *rel*-(6a*R*, 12b*S*) and minor isomer **3aB** the *rel*-(6a*S*, 12b*S*) configuration (see Scheme 3). In both isomers, ring A has a chair and ring B a distorted envelope conformation, and the

Table 2. Crystallographic data for compounds **3a**, **3c**, and **4**.

	3a	**3c**	**4**
Empirical formula	$C_{16}H_{18}ClN$	$C_{17}H_{20}ClN$	$C_{16}H_{12}ClNO$
Formula weight	259.76	273.79	269.72
Temperature (K)	173(2)	173(2)	293(2)
Wavelength (Å)	0.71073	0.71073	0.71073
Crystal size [mm]	$0.77 \times 0.35 \times 0.27$	$0.54 \times 0.35 \times 0.23$	$0.61 \times 0.42 \times 0.15$
Crystal system	orthorhombic	orthorhombic	monoclinic
Space group	*P* bca	*P* bca	$P2_1/c$
a [Å]	9.275(2)	16.4185(13)	9.589(7)
b [Å]	11.370(1)	6.4940(5)	6.376(3)
c [Å]	25.784(3)	26.070(3)	21.256(18)
α [°]	90	90	90
β [°]	90	90	97.90(9)
γ [°]	90	90	90
Volume [Å^3]	2718.9(7)	2779.7(4)	1287(2)
Z	8	8	4
ρ_{ber} [g·cm^{-3}]	1.269	1.308	1.392
μ(Mo-K$_\alpha$) [cm^{-1}]	2.63	2.61	2.86
θ Range [°]	2.71 – 25.94	1.99 – 25.93	2.14 – 25.89
Index ranges	$-11 \le h \le 11$	$-20 \le h \le 19$	$-11 \le h \le 11$
	$-13 \le k \le 13$	$-7 \le k \le 7$	$-7 \le k \le 7$
	$-31 \le l \le 31$	$-32 \le l \le 31$	$-26 \le l \le 25$
Reflections collected	19924	20257	9554
Independent reflections (R_{int})	2562 (0.0383)	2602 (0.0435)	2426 (0.0627)
Completeness of data set [%]	96.6	96.4	96.9
Data / restraints / parameters	2562 / 0 / 172	2602 / 24 / 209	2426 / 0 / 220
Goodness-of-fit on F^2	1.052	1.036	1.034
Final *R* indices [$I > 2\sigma(I)$]; *R*1, *wR*2	0.0378, 0.0984	0.0406, 0.1037	0.0445, 0.1135
R Indices (all data); *R*1, *wR*2	0.0468, 0.1028	0.0596, 0.1110	0.0661, 0.1221
Largest diff. peak and hole [e·Å^{-3}]	0.23, −0.30	0.34, −0.30	0.28, −0.18

rings are trans-fused. This geometry puts both the nitrogen lone pair and the angular hydrogen atom 12b-H in axial positions with respect to the chair conformation of the piperidine ring. It should be noted that the crystal structure analysis revealed only the major differences in shape for the two isomers, *i.e.* the distinctly different positions of atoms C(6)/C(6') and C(7)/C(7'), but not the obviously smaller positional deviations that must be present in other parts of the molecule, in particular in the chlorophenyl moiety. This shortcoming must be attributed to the low occupation factor of the minor isomer.

The ^{1}H and ^{13}C NMR data of the A, B, and C rings of thieno-isoindole derivative **3b** are in close agreement with those of **3a**. However, the diastereomer ratio is reversed. Thus, it can be concluded that **3b** has the same stereochemistry as **3a** and that the two isomers observed correspond to **3bA** (*rel*-(4a*R*, 10b*S*), minor) and **3bB** (*rel*-(4a*S*, 10b*S*), major) (Scheme 3).

The molecular structure of **3c** in the solid state is shown in Fig. 2. Again, a part of the molecule is found to be disordered over two positions. When this disorder is disentangled, it can be seen that both components have the same relative configuration (shown in Fig. 2 is the *rel*-(7a*S*, 13b*R*) configuration), which is identical with the configuration of the major diastereomer of **3a**, but differ in the junction of the A and B rings: These rings are cis-fused in the major component and trans-fused in the minor one. The two stereoisomers can be interconverted by nitrogen inversion accompanied by a conformational change in the azepane ring A (Scheme 3; note that the structural formula for trans-fused **3c** has a mirror image relationship to the molecule plot shown in Fig. 2), and this process must be facile in solution (vide infra).

Spectroscopic data support the crystallographic evidence concerning the A/B ring fusion in compounds **3a – c**. In the IR spectra of all three compounds, medium-strong bands in the range 2700 – 2800 cm^{-1} (Bohlmann bands) indicate the antiperiplanar relationship between the lone pair at nitrogen and the adjacent angular C – H bond [15]. In the ^{1}H NMR spectra, the signal of the angular protons 12b-H (**3a**) and 10a-H (**3b**) is shifted upfield by *ca.* 1 ppm relative to 13b-H (**3c**) (Table 1). These values are again indicative of the trans-junction in the former two cases and compatible with the predominant cis-junction in **3c** which brings

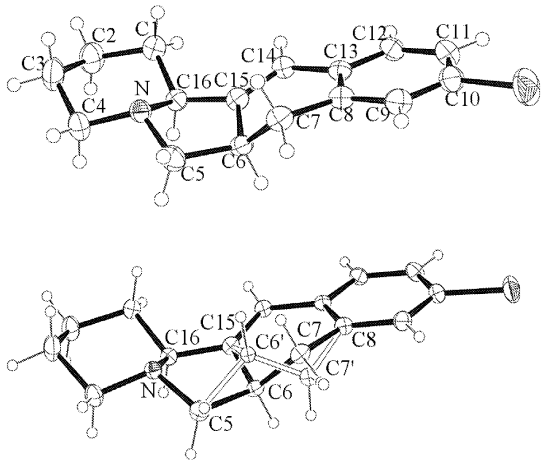

Fig. 1. Molecular structure of **3a** in the solid state: the upper plot shows the major diastereomer **3aA** (ellipsoids shown at 50% probability), and the lower plot (ellipsoids shown at 30% probability) visualizes the disorder found in the crystal where C6' and C7' belong to the minor diastereomer **3aB** (site occupation factors of the disordered parts are 0.87 and 0.13). Torsion angles (°): C4 – N-C16-C1 64.5(2), C5-N-C16-C15 −42.7(1), C5-C6-C15-C16 −14.8(2), C7-C6-C15-C14 40.9.

the angular C – H bond and the nitrogen lone pair in a gauche orientation [6].

For compound **3c**, temperature-dependent ^{1}H NMR spectra (500 MHz) indicated the occurrence of conformational changes, although separate signals of interconverting species could not be obtained when the spectra were recorded at 253 K. When the temperature was lowered from 306 to 253 K, all signals of the A and B rings are subject to changes, of which the following are of particular significance (Table 1): The signal of 13b-H is shifted to lower field by 0.21 ppm and the chemical shift difference for the two protons at C-5 and at C-7 increases by 0.35 and 0.29 ppm, respectively. Bearing in mind the abovementioned criterion, according to which an antiperiplanar orientation between a nitrogen lone pair and an adjacent C – H bond causes a significant upfield shift of the δ(H) value relative to the situation of a gauche relationship, some of these changes are compatible with the equilibrium between the cis-A,B and trans-A,B conformers of **3c** (Scheme 3) and an equilibrium shift towards the major (cis) conformer at lower temperature. Only the upfield shift by 0.14 ppm of one 5-H proton signal at low temperature cannot be derived immediately from an inspection of the solid-state structure since both conformers (Fig. 2) exhibit a very similar antiplanar orientation of 5-H_{ax} and the nitrogen lone pair.

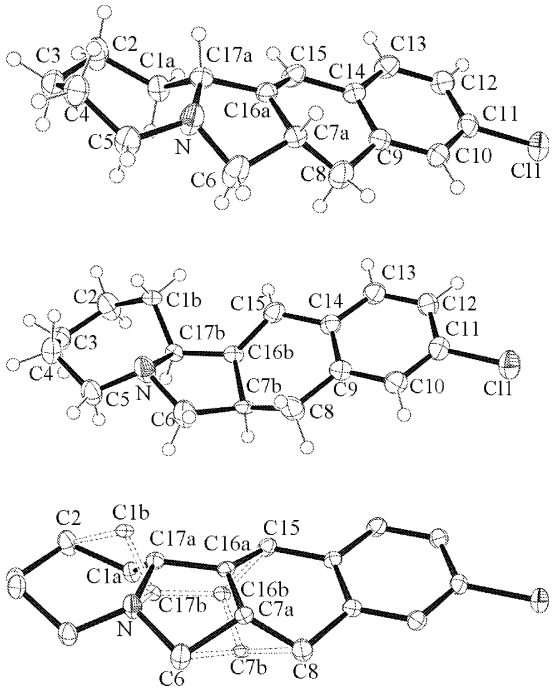

Fig. 2. Molecular structure of **3c** in the solid state. Top and middle: major and minor conformer, site occupation factors 0.75 and 0.25. Bottom: disorder in the solid state showing the partial overlay of the two conformers; the minor conformer is indicated by dashed bonds. Torsion angles (°): C5-N-C17a-C1a −34.1(3), C6-N-C17a-C16a −22.6(3); C5-N-C17b-C1b 85.2(5), C6-N-C17b-C16b −42.6(5).

Compound **3a** was treated with selenium dioxide/pyridine in order to see whether dehydrogenation of ring C could be achieved. Only one product could be isolated in modest yield after chromatographic workup which was identified by 1D and 2D NMR spectra as 8-chloro-5,5a,6,12-tetrahydrobenzo[*g*]pyrrolo[1,2-*b*]isoquinolin-12-one (**4**); a crystal structure analysis confirmed this assignment (Fig. 3). Although **4** was not the expected product, its formation is readily explained taking into account several well known functional group oxidations with SeO_2 [16]: allylic oxidation at C-12b yields a half-aminal which by ring-opening forms an aminoketone; α-oxidation of the latter generates a 1,2-diketone that can undergo cyclocondensation to form a dihydropyrrole ring which is finally dehydrogenated to form a pyrrole ring. Thus, treatment of **3a** with SeO_2 is accompanied by a $(6,5) \rightarrow (5,6)$ ring transformation of the A and B rings. Efforts to improve the yield of **4** failed as even lower yields were obtained when the reaction was carried out in glacial acetic acid or in a dioxane-glacial acetic acid-water mixture.

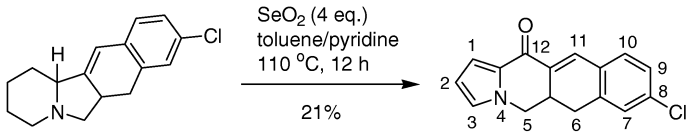

3a **4**

Scheme 4. Oxidative rearrangement of **3a**.

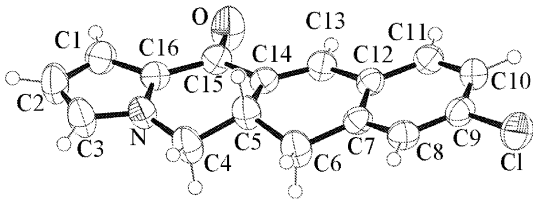

Fig. 3. Molecular structure of **4** in the solid state. Thermal ellipsoids correspond to a 50% probability. Selected bond lengths (Å) and angles (°): N-C3 1.358(3), N-C16 1.374(3), C3-C2 1.374(4), C2-C1 1.385(4), C1-C16 1.383(3), C15-O 1.232(3), C15-C16 1.448(3), C13-C14 1.338(3), C9-Cl 1.748(2); C3-N-C4 127.2(2), C3-N-C16 108.6(2), C4-N-C16 123.8(2).

*Conversion of salts **2a,c,d** into enamines and ring expansion*

Iminium salts can be converted into enamines conveniently by deprotonation with sodium trimethylsilanolate [17]. This transformation is also possible with isoindolium salts **2**; in order to avoid subsequent reaction of the formed enamine with the precursor iminium salt, the latter must be slowly added to the base. In this manner, cyclic enamine **5c** was obtained from iminium salt **2c** (Scheme 5). According to the ^{1}H NMR spectrum of the crude reaction mixture, **5c** was formed in good yield, but much material was lost during chromatographic workup and incomplete crystallization. Therefore, we decided to submit **5c** to the reaction with dimethyl acetylenedicarboxylate (DMAD) in a one-pot procedure. Indeed, the expected two-carbon ring expansion product **6c**, a 4,6,7,9,9a,10-hexahydro-5*H*-azonino[2,1-*a*]benzo[*f*]isoindole, could be isolated in a yield of 63% based on **2c**. In a similar manner, iminium salts **2a** and **2d** were converted into 4,5,6,8,8a,9-hexahydroazocino[2,1-*a*]benzo[*f*]isoindole **6a** and 4a,5,7,8,9,10-hexahydro-4*H*-azonino[2,1-*a*]thieno[3,2-*f*]isoindole **6d**, respectively, without isolation of the intermediate enamine.

Ring expansion products **6** are yellow to orange-red crystalline compounds. Their constitution follows from a comparison of the NMR spectra with those of the precursor salts **2**. The incorporation of the aminodiene moiety is indicated by the additional olefinic carbon signals and a signal for an olefinic proton at $\delta = 6.25$ ppm in **6a** and 6.73 – 6.78 ppm in **6c,d**. The olefinic carbon signals of the enaminoester fragment appear at $\delta = 86.8 - 88.0$ and 133.2 – 135.9 ppm, indicating the polarization of this double bond due to push-pull substitution. The N*C*H$_2$ carbon in the five-membered ring gives rise to a signal at $\delta = 60.0 - 60.8$ ppm, which is almost identical with the values for **3c** and the major isomers of neutral azaheterocycles **3a,b** (Chart 1) and a few ppm upfield relative to iminium salts **2**, where $\delta_{CD_3CN} = 63.7 - 66.1$ ppm [1]. On the other hand, the signal of the N*C*H$_2$ carbon in the eight- or nine-membered ring A is found at $\delta = 44.7 - 45.8$ ppm, 3.6 – 9.4 ppm upfield relative to the values for **2** and **3**. These upfield shifts are probably caused by γ effects in the particular conformations of the medium-sized rings.

The two-carbon ring expansion of enamines of cyclic ketones (*i.e.* 1-(dialkylamino)cycloalkenes) with acetylenic esters has often been applied to the synthesis of medium-sized carbocyclic and heterocyclic compounds (see lit. [18] and cited references), while it seems not to have been widely used to convert cyclic enamines into seven-, eight- and nine-membered azaheterocycles [19 – 21]. It has been shown that [2+2] cycloaddition initially generates cyclobutenes which undergo conrotatory ring opening to form cis,trans-cycloalkadienes [18]. In several cases, subsequent thermal isomerization into cis,cis-cycloalkadienes has been observed. For ring expansion products **6a,c,d**, the cis,cis-configuration of the diene unit can be assumed based on the chemical shift of the olefinic proton (see above), which would appear at higher field ($\delta < 6$ ppm) in the trans,cis-isomer [18]. Furthermore, the cis,cis-diene configuration was established by crystal structure analysis of a compound that is structurally closely related to **6a** and agrees with the latter in the relevant NMR data [22].

Interactions with Double-stranded Nucleic Acids

The stacking of aromatic ligands between nucleobases of double-stranded nucleic acids [23] plays an important role also in the development of new thera-

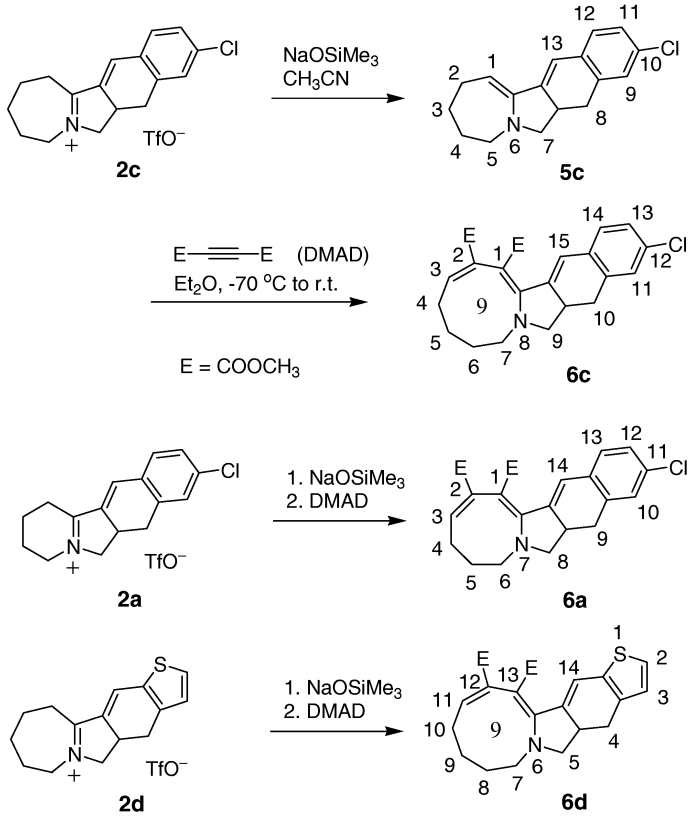

Scheme 5. Ring enlargement of tetracyclic iminium salts **2a,c,d** *via* cyclic enamines.

peutic agents [24]. It was of interest to study the binding of the isoindolium systems of the present paper to nucleic acids; the presence of positive charges and a partially aromatic moiety could allow both binding in the groove or intercalation by stacking. Typical intercalators have extended and rather flat aromatic systems, and are usually characterized by a significant increase ΔT of the double-strand melting temperature [25], and of viscosity due to the polymer strand elongation. Intercalation also occurs with rather small naphthalene and quinolinium systems, bearing a flexible side chain with ammonium groups, as long as the presence of competing cations from the buffer does not weaken the salt bridge between the ammonium groups and the groove phosphate [26].

The partially hydrogenated $[a,f]$-annelated isoindolium salts **2** do not have an extended aromatic chromophor, and the tetracyclic skeleton is not planar but exhibits a rather flat puckered shape (see lit. [1] for the solid-state structure of **2a**). It is known that flatness is not necessarily a stringent requirement for intercalation, such as with e.g. bulky porphyrins [27].

Table 3. Physical measurements related to interactions of DNA with **2a,c**.

DNA melting changes				
Compound		DNA	ΔT_m (°C)	r[a]
2a		CT-DNA	3.5[b] (+1.27[c])	1.0
2c		CT-DNA	3.7[b] (+1.3[c])	1.0
2°		poly(dA – dT)	1.8[b]	1.0
			0.9[b]	0.5
		poly(A – U)	0.0[b]	1.0
2c		poly(dA – dT)	+1.7[b]	1.0
			+0.8[b]	0.5
		poly(A – U)	−0.3[b]	1.0
Viscometry		α		
2		≤ 0.4[b]		
2c		≤ 0.4[b]		
NMR measurements[d]				
Compound		Signal (δ, ppm)	Δ ppm[e]	$\Delta W_{1/2}$ (Hz)[e]
2a	12-H	7.607	−0.25	45
	11-H	7.447	−0.24	41

[a] r = [**2**]/[nucleic acid phosphates]; ΔT_m with **2b** are < 0.7 °C (at $r = 0.5$); [b] MES00: 0.01 M MES (2-(*N*-morpholino)ethanesulfonic acid), 0.001 M EDTA, pH 6.25; [c] PIPES00: 0.01 M PIPES (piperazine *N*,*N*′-bis(2-ethanesulfonic acid)), 0.001 M EDTA, pH 7.0; [d] 0.02 M phosphate buffer, pH 7.0, $T = 298$ K; [e] measured for [nucleic acid phosphates]/[**2a**] = 10:1.

The results of DNA melting behavior and viscometry studies as well as NMR measurements are given in Table 3. The observed small melting changes do not necessarily reflect absence of reaction with double-stranded nucleic acids, as stacking within single strands would well be possible with the isoindolium salts, which is a known way to actually lower stabilities of folded nucleic acids [28a]. Ligands which bind to double-strands but at the same time also strongly to single strands indeed show relatively small melting effects [28b], whereas those which bind significantly only to single strands lead to large melting point **de**crease [28a]. Furthermore, it is known that in particular weakly intercalating ligands are in equilibrium with groove binding modes depending *inter alia* on the presence of *e.g.* buffer cations which can compete with the ligand binding at the groove phosphates [29].

The very small increase in viscosity also does not exclude intercalation, as bending of the double strand can lower the apparent length [30]. Clear evidence for intercalation has been said to require a number of methods [31]. For the present investigation we have used a NMR method, which demonstrates intercalation by observation of ligand proton signals [32]. Intercalation is usually characterized by upfield shifts between 0.1 and 1 ppm [32], produced by the ring current effects of the nucleobases on the ligand, and by simultaneous line broadening by usually 20 – 50 Hz resulting from tumbling time changes due to fixation of the ligand within the helix. On the other hand, some shielding effects have also been reported for ligands which at least for the most part do not intercalate [33]. Nevertheless, it is remarkable that only the aromatic protons of **2** showed shielding by 0.25 ppm, and distinct line width increase by 41 to 45 Hz. This suggests that the chlorophenyl part of the system is at least partially intercalated within the double-strand, but also would be in line with stacking within unfolded helical parts. Clearer evidence for the binding mechanism would require further studies which were not in the scope of the present investigation.

Experimental Section

General Methods. The NMR spectra were taken on a Bruker AMX 500 (^{1}H: 500.14 MHz; ^{13}C: 125.77 MHz) instrument. For the ^{1}H NMR spectra, tetramethylsilane was used as the internal standard whereas the solvent signal was used as standard in the ^{13}C NMR spectra [$\delta(CD_3CN)$ = 1.3 ppm]; pt = pseudotriplet, mc = centered multiplet). The signal assignment was based on proton-coupled ^{13}C spectra, H,H COSY, and C,H (^1J) as well as C,H (^2J, ^3J) correlation spectra. IR spectra were recorded on a Perkin Elmer IR 883 spectrometer. Column chromatography was performed using hydrostatic pressure (silica gel 60, Macherey-Nagel, 0.063 – 0.2 mm) Microanalyses were carried out in the Division of Analytical Chemistry of the University of Ulm with analyser systems Elementar Vario E1 and Heraeus CHN rapid. Melting points were determined in an apparatus after Dr. Tottoli (Buechi) and are not calibrated. Solvents were dried by standard methods and were stored under an argon atmosphere. The petroleum ether used had a boiling point range of 40 – 60 °C. The tetracyclic iminium triflates **2a – d** were prepared as described [1] from propyne iminium triflates **1a – c** [34].

*(±)-rel-(6aR, 12bS)- and rel-(6aS, 12bS)-9-Chloro-1,2,3,4, 6,6a,7,12b-octahydrobenzo[f]pyrido[2,1-a]isoindole (**3a**)*

To a magnetically stirred solution of isoindolium triflate **2a** (1.22 g, 3.0 mmol) in THF (15 ml), cooled at 0 °C, $LiAlH_4$ (0.114 g, 3.0 mmol) was slowly added. After stirring for 1 h at r. t., the mixture was hydrolyzed by careful addition of water (20 ml), the precipitate was filtered off with suction and the residual solution was extracted with CH_2Cl_2 (3 × 30 ml). The organic phases were combined, and the solvent was evaporated. The residue was separated by column chromatography (CH_2Cl_2-EtOAc, 1:1). Crystallization from acetone-petroleum ether furnished **3a** (0.53 g, 67%) as colorless crystals, m.p. 103 – 104 °C. According to ^{1}H NMR, a 72:28 mixture of isomers **A** (*rel*-(6a*R*, 12b*S*-**3a**)) and **B** (*rel*-(6a*S*, 12b*S*-**3a**)) was obtained. Fractionating crystallization of this mixture from acetonitrile-acetone gave first a crystal batch which was a 82:18 mixture of **A** and **B**, followed by a 25:75 mixture of **A** and **B**. – IR (KBr): ν = 2934 (s), 2884 (m), 2849 (m), 2813 (m), 2779 (m), 2752 (w), 2706 (w), 1594 (w), 1557 (w), 1479 (m) cm^{-1}. – ^{1}H NMR: Table 1. – ^{13}C NMR: Chart 1. – Analysis for $C_{16}H_{18}ClN$ (259.78): calcd. C 73.98, H 6.98, N 5.39; found C 73.41, H 6.86, N 5.36.

*(±)-rel-(4aR, 10aS)- and rel-(4aS, 10aS)-4,4a,5,7,8,9,10, 10a-Octahydropyrido[2,1-a]thieno[3,2-f]isoindole (**3b**)*

The reaction was carried out starting from **2b** (0.38 g, 1.0 mmol) and $LiAlH_4$ (0.038 g, 1.0 mmol) as described for **3a**. Crystallization from acetone-petroleum ether furnished **3b** as a pale-yellow solid (0.14 g, 58%), m.p. 97 – 98 °C. According to ^{1}H NMR, a 17:83 mixture of (*rel*-(4a*R*, 10a*S*-**3b**)) and (*rel*-(4a*S*, 10a*S*-**3b**)) was obtained. – IR (KBr): ν = 2922 (s), 2851 (m), 2822 (m), 2773 (s), 2738 (m), 2701 (m), 1640 (w) cm^{-1}. – ^{1}H NMR: Table 1. – ^{13}C NMR: Chart 1. – Analysis for $C_{14}H_{17}NS$ (231.36): calcd. C 72.68, H 7.41, N 6.05; found C 72.31, H 7.30, N 5.92.

*(±)-rel-(7aS, 13bR)-10-Chloro-2,3,4,5,7,7a,8,13b-octahydro-1H-azepino[f]pyrido[2,1-a]isoindole (**3c**)*

The reaction was carried out starting from **2c** (0.84 g, 2.0 mmol) and $LiAlH_4$ (0.076 g, 2.0 mmol) as described for **3a**. Crystallization afforded **3c** (0.38 g, 69%) as colorless crystals, m.p. 108 °C. – IR (KBr): $\nu = 3023$ (s), 2929, 2875, 2843 (all m), 2798 (m), 2744 (m), 1474 (m) cm^{-1}. – ^1H NMR: Table 1. – ^{13}C NMR: Chart 1. – Analysis for $C_{17}H_{20}ClN$ (273.81): calcd. C 74.57, H 7.36, N 5.12; found C 73.96, H 7.10, N 4.97.

*8-Chloro-5,5a,6,12-tetrahydrobenzo[g]pyrrolo[1,2-b]isoquinolin-12-one (**4**)*

A solution of isoindole **3a** (0.390 g, 1.5 mmol) and SeO_2 (0.666 g, 6.0 mmol) in toluene-pyridine (1:1, 20 ml) was heated for 12 h at reflux. The solvent was evaporated and the residue was treated with CH_2Cl_2-water. The water phase was extracted with CH_2Cl_2 (3×30 ml), the organic phases were combined, and the solvent was evaporated. The residue was separated first by flash chromatography (CH_2Cl_2), followed by chromatography on a Merck Lobar column (silica gel, CH_2Cl_2-methanol 98 : 2 → 95 : 5). Pure **4** (0.086 g, 21%) was obtained as light-yellow crystals by crystallization from $CHCl_3$-petroleum ether; m.p. 225 °C. – IR (KBr): $\nu = 3026$ (w), 2962 (w), 1646 (s), 1597 (s), 1474 (m), 1262 (s) cm^{-1}. – ^1H NMR ($CDCl_3$): $\delta = 2.79$ (pt, 1 H, 6-H), 2.97 (dd, $^2J = 15.5$ Hz, $^3J = 6.3$ Hz, 1 H, 6-H), 3.32 (mc, 1 H, 5a-H), 3.86 (pt, 1 H, 5-H), 4.42 (dd, $^2J = 14.2$ Hz, $^3J = 6.0$ Hz, 1 H, 5-H), 6.33 (dd, $^3J = 4.0$ Hz, $^3J = 2.4$ Hz, 1 H, 2-H), 6.91 (mc, 1 H, 3-H), 7.14 (dd, $^3J = 4.0$ Hz, $^4J = 1.4$ Hz, 1 H, 1-H), 7.16 – 7.28 (m, 3 H, 7-H, 9-H, 10-H), 7.73 (d, $^4J = 2.7$ Hz, 1 H, 11-H). – ^{13}C NMR ($CDCl_3$): $\delta = 31.1$ (d, C-5a), 32.3 (t, C-6), 49.2 (t, C-5), 111.2 (d, C-2), 115.5 (d, C-1), 126.1 (d, C-3), 127.5 (d, C-9), 127.7 (d, C-7), 130.4 (d, C-10), 131.1 (d, C-10a), 131.6 (s, C-12a), 132.6 (s, C-11), 135.3 (s, C-8), 136.6 (s, C-6a), 175.2 (s, C-12); the signal of C-11a was not found.

*10-Chloro-2,4,5,7,7a,8-hexahydro-3H-azepino[2,1-a]benzo[f]isoindole (**5c**)*

A solution of salt **2c** in acetonitrile (20 ml) was added to a suspension of sodium trimethylsilanolate (0.224 g, 2.2 mmol) in acetonitrile (30 ml), and the mixture was stirred for 1 h. The solvent was evaporated at 0.01 mbar, and from the residue a yellow oil was extracted with pentane (3×50 ml) which was dissolved in CH_2Cl_2. Petroleum ether was added until the solution became turbid and after a while, **5c** separated in the form of light-yellow crystals (0.196 g, 36%), m. p. 143 °C. – IR (KBr): $\nu = 3014$ (w), 2928 (m), 1646 (m), 1473 (m) cm^{-1}. – ^1H NMR ($CDCl_3$): $\delta = 1.18$ – 1.31 (m, 1 H, 3-H^A), 1.47 – 1.60 (m, 1 H, 4-H^A), 1.84 – 1.96 (m, 2 H, 3-H^B, 4-H^B), 2.12 (pt, 1 H, 2-H^A), 2.36 – 2.47 (m, 1 H, 2-H^B), 2.51 – 2.64 (m, 2 H, 5-H^A, 8-H^A), 2.73 (pt, 1 H, 7-H^A), 2.87 (dd, $^2J = 15.0$, $^3J = 6.6$ Hz, 1 H, 8-H^B), 2.90 – 3.05 (m, 1 H, 7a-H), 3.22 – 3.30 (m, 1 H, 5-H^B), 3.56 (pt, 1 H, 7-H^B), 5.22 (s, 1 H, 1-H), 6.49 (d, $^4J = 2.6$ Hz, 1 H, 13-H) 6.97 (d, $^3J = 8.0$ Hz, 1 H, 12-H), 7.06 – 7.13 (m, 2 H, 9 H, 11-H). – ^{13}C NMR ($CDCl_3$): $\delta = 27.6$ (t, C-3), 28.8 (t, C-2), 29.9 (t, C-4), 32.8 (t, C-8), 36.2 (d, C-7a), 54.0 (t, C-5), 61.4 (t, C-7), 98.8 (d, C-1) 113.3 (d, C-13), 126.7 (d, C-11), 127.2 (d, C-12), 127.7 (d, C-9), 131.4 (s, C-10), 133.7 (s, C-12a), 135.9 (s, C-8a), 143.7 (s, C-13a), 145.8 (s, C-13b). – Analysis for $C_{17}H_{18}ClN$ (271.79): calcd. C 75.13, H 6.68, N 5.15; found C 74.84, H 6.53, N 5.09.

*Dimethyl 11-chloro-4,5,6,8,8a,9-hexahydroazocino[2,1-a]benzo[f]isoindole-1,2-dicarboxylate (**6a**)*

A solution of salt **2a** (0.408 g, 1.0 mmol) in acetonitrile (10 ml) was added during 3 h to a suspension of sodium trimethylsilanolate (0.112 g, 1.1 mmol) in acetonitrile (10 ml). The mixture was stirred for one additional hour, and the solvent was removed at 0.01 mbar. The residue was extracted with pentane (3×50 ml), the pentane extracts were combined, and the solvent was evaporated. The remaining yellow oil was dissolved in ether (20 ml), and after cooling to −70 °C, freshly distilled dimethyl acetylenedicarboxylate (0.14 ml, 1.1 mmol) was added. The reaction mixture was brought to room temperature over a period of 12 h (acetone/dry ice bath). The solvent was removed at 0.01 mbar, and the remaining foam-like residue was submitted to column chromatography (CH_2Cl_2 as eluent). Compound **6a** was isolated and recrystallized from acetone–petroleum ether, yielding 0.172 g (43%) of a yellow solid, m. p. 234 °C. – IR (KBr): $\nu = 1713$ (s), 1640 (w), 1537 (s), 1263 (s), 1247 (s), 1216 (s), 1104 (s) cm^{-1}. – ^1H NMR ($CDCl_3$): $\delta = 1.05$ – 1.17 (m, 1 H, 5-H^A), 1.64 – 1.78 (m, 1 H, 5-H^B), 2.15 – 2.26 (m, 1 H, 4-H^A), 2.42 – 2.65 (m, 2 H, 4-H^B, 9-H^A), 2.96 – 3.15 (m, 4 H, 6-H^A, 8-H^A, 8a-H, 9-H^B), 3.49 – 3.60 (m, 1 H, 8-H), 3.67 (s, 3 H, OMe), 3.75 (s, 3 H, OMe), 4.07 (pt, 1 H, 6-H), 6.25 (dd, $^3J = 9.9$, $^3J = 7.1$ Hz, 1 H, 3-H), 6.84 (s, 1 H, 14-H), 7.05 (d, $^3J = 7.9$ Hz, 1 H, 13-H), 7.09 – 7.22 (m, 2 H, 10-H, 12-H). – ^{13}C NMR ($CDCl_3$): $\delta = 11.8$ (t, C-5), 24.3 (t, C-4), 32.8 (t, C-9), 33.7 (d, C-8a), 44.7 (t, C-6), 51.1 (q, Me), 51.9 (q, Me), 60.0 (t, C-8), 88.0 (s, C-1), 126.1 (d, C-14), 127.4 (d, C-12), 127.6 (d, C-10), 128.7 (d, C-13), 132.3 (s, C-13a), 132.5 (d, C-3), 133.3 (s, C-11), 135.4 (s, C-9a), 135.9 (s, C-2), 139.6 (s, C-14a), 154.1 (s, C-14b), 169.3 (s, CO_2Me), 171.2 (s, CO_2Me). – Analysis for $C_{22}H_{22}ClNO_4$ (399.87): calcd. C 66.08, H 5.55, N 3.50; found C 65.81, H 5.64, N 3.36.

*Dimethyl 12-chloro-4,6,7,9,9a,10-hexahydro-5H-azonino-[2,1-a]benzo[f]isoindole-1,2-dicarboxylate (**6c**)*

The synthesis was carried out as described for **6a**, from salt **2c** (0.422 g, 1.0 mmol), $NaOSiMe_3$ (0.112 g, 1.1 mmol)

and dimethyl acetylenedicarboxylate (0.14 ml, 1.1 mmol); yield: 0.259 g (63%); orange-red crystals, m. p. 230 °C. – IR (KBr): $\nu = 1713$ (vs), 1682 (s), 1536 (s), 1277 (s), 1249 (s), 1104 (s) cm^{-1}. – ^1H NMR ($CDCl_3$): $\delta = 1.82 - 2.06$ (m, 4 H, 5-H, 6-H), 2.13 – 2.32 (m, 2 H, 4-H), 2.61 (pt, 1 H, 10-H^A), 2.84 – 2.92 (m, 1 H, 7-H), 3.05 – 3.15 (m, 2 H, 9a-H, 10-H^B), 3.32 – 3.39 (m, 1 H, 9-H), 3.60 – 3.68 (m, 1 H, 9-H), 3.66 (s, 3 H, OMe), 3.75 (s, 3 H, OMe), 4.21 – 4.29 (m, 1 H, 7-H), 6.78 (dd, $^3J = 12.0$, $^3J = 6.1$ Hz, 1 H, 3-H), 6.99 (d, $^4J = 2.8$ Hz, 1 H, 15-H), 7.09 (d, $^3J = 8.0$ Hz, 1 H, 14-H), 7.12 – 7.19 (m, 2 H, 11-H, 13-H). – ^{13}C NMR ($CDCl_3$): $\delta = 23.0$ (t, C-5), 24.1 (t, C-6), 26.4 (t, C-4), 33.1 (t, C-10), 33.7 (d, C-9a), 45.8 (t, C-7), 50.9 (q, Me), 51.9 (q, Me), 60.8 (t, C-9), 87.7 (s, C-1), 126.5 (d, C-15), 127.1 (d, C-13), 127.6 (d, C-11), 128.8 (d, C-14), 132.4 (s, C-14a), 133.2/133.3 (2 s, C-2, *C*Cl), 135.6 (s, C-10a), 139.7 (s, C-15a), 140.7 (d, C-3), 156.6 (s, C-15b), 169.3 (s, *C*O_2Me), 170.7 (s, *C*O_2Me). – Analysis for $C_{23}H_{24}ClNO_4$ (413.90): calcd. C 66.74, H 5.84, N 3.38; found C 66.40, H 5.71, N 3.29.

*Dimethyl 4a,5,7,8,9,10-hexahydro-4H-azonino[2,1-a]-thieno[3,2-f]isoindole-12,13-dicarboxylate (***6d***)*

The synthesis was carried out as described for **6a**, from salt **2d** (0.394 g, 1.0 mmol), $NaOSiMe_3$ (0.112 g, 1.1 mmol) and dimethyl acetylenedicarboxylate (0.14 ml, 1.1 mmol); yield: 0.248 g (64%); red-orange crystals, m. p. 216 °C. – IR (KBr): $\nu = 1714$ (vs), 1681 (s), 1532 (s), 1242 (vs), 1215 (s), 1105 (s) cm^{-1}. – ^1H NMR ($CDCl_3$): $\delta = 1.84 - 2.09$ (m, 4 H, 8-H, 9-H), 2.16 – 2.30 (m, 2 H, 10-H), 2.49 (pt, 1 H, 4-H^A), 2.87 – 2.95 (m, 1 H, 7-H^A), 3.13 – 3.25 (m, 2 H, 4-H^B, 4a-H), 3.36 (t, 1 H, 5-H^A), 3.61 – 3.70 (m, 1 H, 5-H^B), 3.65 (s, 3 H, OMe), 3.75 (s, 3 H, OMe), 4.19 – 4.28 (m, 1 H, 7-H^B), 6.73 (dd, ^3J = 12.0, $^3J = 6.1$ Hz, 1 H, 11-H), 6.90 (d, $^3J = 4.9$ Hz, 1 H, 3-H), 7.15 (d, $^4J = 2.0$ Hz, 1 H, 14-H), 7.23 (d, $^3J = 4.9$ Hz, 1 H, 2-H). – ^{13}C NMR: $\delta = 22.8$ (t, C-9), 23.6 (t, C-8), 26.2 (t, C-10), 29.1 (t, C-4), 34.6 (d, C-4a), 45.8 (t, C-7), 50.9 (q, Me), 51.9 (q, Me), 60.6 (t, C-5), 86.8 (s, C-13), 121.3 (d, C-14), 125.3 (d, C-2), 126.7 (d, C-3), 133.6 (s, C-12), 134.8 (s, C-3a), 135.1 (s, C-14a), 135.5 (s, C-13b), 139.8 (d, C-11), 157.2 (s, C-13a), 169.6 (s, *C*O_2Me), 170.6 (s, *C*O_2Me). – Analysis for $C_{21}H_{23}NO_4S$ (385.48): calcd. C 65.43, H 6.01, N 3.63; found C 65.34, H 6.01, N 3.52.

X-ray crystal structure determinations

Data collection was performed on an imaging-plate diffractometer (STOE IPDS) using monochromatized Mo-K_α radiation. The structures were solved by direct methods and refined by a full-matrix least-squares procedure based on F^2 values using the program package SHELX-97 [35]. Hydrogen atom positions were calculated and refined by the riding model. Crystallographic data and refinement details are given in Table 2.

Crystals of compound **3a** were obtained by two fractionating crystallizations from acetonitrile-ether (85:15 mixture of isomers **A** and **B**, see above). It was found that the positions of atoms C(6) and C(7) are disordered; refinement of site occupation factors gave values of 0.87 and 0.13. The atoms on the minor sites were refined only isotropically, but the position of C(6') did not turn out accurately as seen from the bond geometry. Although the presence of a second stereoisomer would require that in addition to C(6) and C(7) further atom positions, in particular in the chlorophenyl moiety, are disordered, no additional peaks were found in the final difference Fourier map.

Crystals of **3c** were obtained from a mixture of acetonitrile, dichloromethane and acetone. A portion of the molecule with four contiguous atoms (C(1), C(17), C(16), C(7)) was found disordered over two sites with occupation factors 0.75 and 0.25. It is expected that this disorder slightly affects also the atoms adjacent to this fragment, but no resolved peaks corresponding to the minor component could be detected in these cases. However, the hydrogen positions at these atoms (C(2), C(7), C(8)) were calculated for both isomers and included in the refinement.

Crystallographic data have been deposited as CCDC-229645 (**3a**), -229646 (**3c**), and -229647 (**4**). These data can be obtained free of charge *via* http://www.ccdc.cam.ac.uk/conts/retrieving.html (or from the Cambridge Crystallographic Data Centre, 12, Union Road, Cambridge CB2 1EZ, UK; fax: (+44)1223-336-033.

DNA Binding Studies

Solutions

MES00 buffer contained 0.01 M MES00 (2-(*N*-morpholino)ethanesulfonic acid), 0.001 M EDTA, adjusted to pH = 6.25 ($I = 0.01$ M); PIPES00 buffer contained 0.01 M PIPES (1,4-piperazine-bis(2-ethanesulfonic acid)), 0.001 M EDTA, adjusted to pH = 7.0 ($I = 0.02$ M). The phosphate buffer used for NMR measurements contained 0.02 M Na_2HPO_4 in D_2O, adjusted to pH = 7.0 (pD = 7.4).

For melting, NMR and viscometry experiments calf thymus(CT)-DNA (Aldrich) was dissolved in the respective buffer, sonicated and filtered through a 0.45 μm filter. PolydA-polydT and polyA-polyU (both from Sigma) were dissolved in MES00 buffer and their phosphate concentrations were determined spectrophotometrically at $\lambda = 260$ nm using $\varepsilon = 6600$ l/mol·cm for CT-DNA and 6000 l/mol·cm for the polymers [29f]. The concentrations of the stock solutions of the ligands were $1 - 2 \cdot 10^{-2}$ mol/l (in DMSO or [D_6]-DMSO (NMR)).

Thermal melting curves

Thermal melting experiments for DNA, RNA and their complexes were carried out as previously described [29f] by following the absorption change at 260 nm as a function of temperature (heating rate of 0.5 °C/min), with a Cary 1 Bio UV-vis spectrophotometer (Varian) connected to a temperature-controller (Varian) and interfaced to a PC. Experimental concentrations for CT-DNA were $\approx 8 \cdot 10^{-5}$ mol/l for polydA*polydT, and polyA*polyU $\approx 4 \cdot 10^{-5}$ mol/l. The absorbance of the ligands was subtracted from every curve, and the absorbance scale was normalized. T_m values are the midpoints of the transition curves, determined from the maximum of the first derivative or graphically by a tangent method [25]. ΔT_m values were calculated subtracting T_m of the free nucleic acid from T_m of complex. Every ΔT_m value here reported was the average of at least two measurements, the deviations in ΔT_m were $< \pm 0.5$ °C.

Viscometry measurements

Viscometric measurements were conducted in an automatic Ubbelohde micro viscometer system (Schott) as previously described [29]. The concentration of CT-DNA in MES00 buffer was $5 \cdot 10^{-4}$ M in phosphates, the ligand to DNA phosphate ratio r less than 0.15. The dilution including addition of DMSO never exceeded 5% and was corrected for in the calculations as well as the viscometry data were corrected for DMSO content due to addition of the ligand stock solutions (final content not exceeding 5% of the total volume). The flow times were measured at least five times with a deviation of ± 0.02 s. The viscosity index α was obtained from the flow times at varying r according to eqn. (1) [36], where t_0, t_{DNA} and t_r denote the flow times of buffer, free DNA and DNA complex at reagent/phosphate ratio r, respectively; L/L_0 is the relative DNA lengthening:

$$L/L_0 = [(t_r - t_0)/(t_{DNA} - t_0)]^{1/3} = 1 + \alpha \cdot r \quad (1)$$

The L/L_0 to r plot was fitted to a straight line that gave slope α. The error in α is ± 0.1.

NMR spectra with CT-DNA were obtained as previously described [29f, 32a] with a ligand concentration of 1 mM. Titrations were conducted adding aliquots of CT-DNA (in 20 mM phosphate buffer) over a range of drug-DNA phosphate ratios r of 1.0 to 10.0. Samples were referenced to TMS as external standard. The line broadening was set to 10 Hz in all spectra to improve the signal-to-noise ratio. The line broadening increase was determined subtracting the width of the signals at half height in the spectrum without DNA from those in the spectra with DNA. Errors in Δppm (at $r = 10.0$): ± 0.005 ppm, in $\Delta W_{1/2}$: ± 10 Hz.

Acknowledgements

This work was supported in Ulm and Saarbrücken financially by the Deutsche Forschungsgemeinschaft. A graduate fellowship to H.-G. H. by the State of Baden-Württemberg is gratefully acknowledged.

[1] H.-G. Herz, J. Schatz, G. Maas, J. Org. Chem. **66**, 3176 (2001).
[2] T. Hartmann, L. Witte, in S. W. Pelletier (ed.): Alkaloids: Chemical and Biological Perspectives, Vol. 9, p. 155, Pergamon, Oxford (1995).
[3] A. D. Elbein, R. J. Molyneux, in S. W. Pelletier (ed.): Alkaloids: Chemical and Biological Perspectives, Vol. 3, chapter 1, Wiley-Interscience, New York (1987).
[4] J. P. Michael, in G. A. Cordell (ed.): The Alkaloids. Chemistry and Biology, Vol. 55, p. 91, Academic Press, New York (2001).
[5] K. A. Tehrani, M. D'hooghe, N. De Kimpe, Tetrahedron **59**, 3099 (2003).
[6] T. A. Crabb, A. R. Katritsky, Adv. Heterocycl. Chem. **36**, 3 (1984).
[7] A. M. Belostotskii, E. Markevich, J. Org. Chem. **68**, 3055 (2003).
[8] T. A. Crabb, R. F. Newton, D. Jackson, Chem. Rev. **71**, 109 (1971).
[9] J. M. McIntosh, L. C. Matassa, J. Org. Chem. **53**, 4452 (1988).
[10] T. A. Crabb, O. G. Roch, J. Chem. Soc., Perkin Trans. 2, 949 (1992).
[11] G. Memetzidis, L. Jung, J.-F. Stambach, Heterocycles **36**, 107 (1993).
[12] a) W. Meise, C. Arth, D. Zlotos, M. Jansen, C. Feldmann, Liebigs Ann. Chem. 1135 (1994); b) W. Meise, D. Zlotos, M. Jansen, N. Zoche, Liebigs Ann. Chem. 567 (1995); c) M. Clemens, W. Meise, K. Himmel, M. Jansen, Liebigs Ann./Recueil 447 (1997); d) D. P. Zlotos, W. Meise, Heterocycles **45**, 2137 (1997).
[13] G. Maas, B. Manz, T. Mayer, U. Werz, Tetrahedron **55**, 1309 (1999).
[14] C. J. Roxburgh, Tetrahedron **50**, 13199 (1994).

[15] F. Bohlmann, Chem. Ber. **91**, 2157 (1958).
[16] A. Krief, L. Hevesi, Organoselenium Chemistry I, Springer, Berlin Heidelberg New York (1988).
[17] M. Glaser, R. Reinhard, G. Maas, Synlett 627 (1994).
[18] a) D. N. Reinhoudt, W. Verboom, G. W. Visser, W. P. Trompenaars, S. Harkema, G. J. van Hummel, J. Am. Chem. Soc. **106**, 1341 (1984); b) G. J. M. Vos, P. H. Benders, D. N. Reinhoudt, R. J. M. Egberink, S. Harkema, G. J. van Hummel, J. Org. Chem. **51**, 2004 (1986).
[19] P. A. Evans, A. B. Holmes, Tetrahedron **47**, 9131 (1991).
[20] 1,2,3,4-Tetrahydro-azocines: P. Sanna, A. Carta, G. Paglietti, J. Chem. Res. Synop. 16 (1992).
[21] Dihydroazepines: a) H. Wamhoff, G. Hendrikx, Chem. Ber. **118**, 863 (1985); b) H. Wamhoff, Adv. Heterocycl. Chem. **38**, 299 (1985).
[22] H.-G. Herz, doctoral thesis, University of Ulm (1999).
[23] Recent review: F. Gago, Methods – A Companion to Methods in Enzymology **14**, 277 (1998).
[24] Recent reviews: M. F. Brana, M. Cacho, A. Gradillas, B. de Pascual-Teresa, A. Ramos, Current Pharm. Design **7**, 1745 (2001); G. Bischoff, S. Hoffmann, Current Med. Chem. **9**, 321 (2002).
[25] a) W. D. Wilson, F. A. Tanious, M. Fernandez-Saiz, C. T. Rigl, Evaluation of Drug/Nucleic Acid Interactions by Thermal Melting Curves; in K. R. Fox (ed.): Methods in Molecular Biology, Vol. 90, Drug-DNA Interaction Protocols: Humana Press Inc., Totowa, N. Y. (1980); b) W. D. Wilson, L. Ratmeyer, M. Zhao, L. Strekowski, D. Boykin, Biochemistry **32**, 4098 (1993); c) L. Kibler-Herzog, B. Kell, G. Zon, K. Shinozuka, S. Mizan, W. D. Wilson, Nucleic Acids Res. **18**, 3545 (1990).
[26] J. Sartorius, H.-J. Schneider, J. Chem. Soc., Perkin Trans. 2, 2319 (1997).
[27] S. A. Bejune, A. H. Shelton, D. R. McMillin, Inorg. Chem. **42**, 8465 (2003); A. B. Guliaev, N. B. Leontis, Biochemistry **38**, 15425 (1999), and references cited therein.
[28] a) A. Ali, M. Gasiorek, H.-J. Schneider, Angew. Chem. **110**, 3183 (1998); Angew. Chem. Int. Ed. **37**, 3016 (1998); b) I. Piantanida, B. S. Palm, P. Cudic, M. Žinič, H.-J. Schneider, Tetrahedron Lett. **42**, 6779 (2001).
[29] a) Lit. [25]; b) lit. [26]; c) J. Kapuscinski, Z. Darzynkiewicz, J. Biomol. Struct. Dyn. **5**, 127 (1987); d) M. Dourlent, C. Hélène, Eur. J. Biochem. **23**, 86 (1971); e) H. W. Zimmermann, Angew. Chem. Int. Ed. **25**, 115 (1986); f) B. S. Palm, I. Piantanida, M. Žinič, H.-J. Schneider, J. Chem. Soc., Perkin Trans. 2, 385 (2000).
[30] a) See also: K. E. Reinert, C. Zimmer, F. Arcamone, J. Biomol. Struct. **14**, 245 (1996); b) Z. Balcarová, V. Kleinwächter, J. Koudelka, G. Löber, K. E. Reinert, L. P. G. Wakelin, M. J. Waring, Biophys. Chem. **8**, 27 (1978); c) K. E. Reinert, J. Mol. Biol. **72**, 593 (1972).
[31] E. C. Long, J. K. Barton, Acc. Chem. Res. **23**, 271 (1990).
[32] a) J. Sartorius, H.-J. Schneider, FEBS Letters, **374**, 387 (1995); b) lit. [29f]; c) S. Chandrasekaran, S. Kusuma, D. W. Boykin, W. D. Wilson, Magn. Reson. Chem. **24**, 630 (1986); d) L. Strekowski, J. L. Mokrosz, W. D. Wilson, M. J. Mokrosz, A. Strekowski, Biochemistry **31**, 10802 (1992).
[33] F. A. Tanious, J. Spychala, A. Kumar, K. Greene, D. W. Boykin, W. D. Wilson, J. Biomol. Struct. Dynam. **11**, 1063 (1994).
[34] R. Neumann, H.-G. Herz, G. Maas, J. Prakt. Chem. **341**, 121 (1999).
[35] G. M. Sheldrick, SHELX-97 – Program for the solution and refinement of crystal structures from diffraction data, University of Göttingen, Germany (1997).
[36] G. Cohen, H. Eisenberg, Biopolymers **8**, 45 (1969); M. Wirth, O. Buchardt, T. Koch, P. E. Nielsen, B. Nordén, J. Am. Chem. Soc. **110**, 932 (1988).